



## Modeling of an engineering method for calculating the thermal stability of walls with a shielded external surface

Zhangabay N.Zh. \* <sup>1</sup> , Giyasov A.I. <sup>2</sup> , Zhangabay A.Zh. <sup>3</sup> ,  
Kolesnikov A.S. <sup>1</sup> , Utelbayeva A.B. <sup>1</sup> 

<sup>1</sup> M. Auezov South Kazakhstan University, Kazakhstan,

<sup>2</sup> Moscow State University of Civil Engineering (MGSU), Russia,

<sup>3</sup> Satbayev University, Kazakhstan

**Abstract.** This paper presents a modeling methodology for an engineering calculation of the thermal stability of external walls with a shielded outer surface forming a ventilated façade system. The objective of the study is to develop a practical design tool for assessing the amplitude attenuation and phase shift of the internal surface temperature under daily climatic fluctuations. The method is based on the solution of a one-dimensional transient heat conduction problem for a multilayer structure subjected to periodic climatic effects. The external boundary condition is defined through an equivalent heat transfer formulation that accounts for shortwave solar radiation, longwave radiative exchange between the screen and the ambient environment, convective heat transfer, and possible ventilation of the air cavity. An engineering calculation algorithm is proposed that incorporates the effect of equivalent solar loading and harmonic variations of outdoor air temperature with high amplitudes of environmental and near-wall air layer fluctuations. A numerical procedure is provided for the “screen – air gap” subsystem, followed by the evaluation of internal surface temperature attenuation and transient heat transfer characteristics. Validation against numerical simulations and experimental data demonstrates a deviation not exceeding 5-10%. The results indicate a significant influence of screen reflectivity, air gap ventilation intensity, and wall heat capacity on improving thermal stability and reducing heat gains during the hot season. The proposed enhanced assessment algorithm can be widely applied in design practice, including the selection of thermal insulation thickness for building envelopes in southern regions, the determination of design loads for ventilation and air-conditioning systems, and the evaluation of indoor thermal conditions under intermittent heating and ventilation regimes. The practical significance lies in the ability to optimize façade system parameters with shielded external surfaces to prevent overheating and improve building energy efficiency. The study is conducted within the framework of ensuring thermal safety of buildings in warm climate conditions.

**Keywords:** thermal stability, transient heat transfer, shielded surface, ventilated façade, phase shift, attenuation coefficient, radiative-convective heat transfer, life safety

\*Corresponding author E-mail: [Nurlan.Zhanabay777@mail.ru](mailto:Nurlan.Zhanabay777@mail.ru)

**Please cite this article as:** Zhangabay N.Zh., Giyasov A.I., Zhangabay A.Zh., Kolesnikov A.S., Utelbayeva A.B. Modeling of an engineering method for calculating the thermal stability of walls with a shielded external surface. Construction Materials and Products. 2026. 9 (2). 6. DOI: 10.58224/2618-7183-2026-9-2-6

---

## 1. INTRODUCTION

Under conditions of increasing solar heat gains and elevated outdoor air temperatures, the risk of envelope overheating and subsequent indoor thermal discomfort significantly increases. As a result, building systems with shielded external surfaces forming ventilated façade configurations are becoming increasingly relevant. However, widely used regulatory and simplified steady-state calculation methods, as well as standard dynamic thermal stability models, insufficiently describe the combined shortwave and longwave radiation exchange, convective heat transfer, and air – structure interaction within the “screen – air gap – structural wall” subsystem. This limitation restricts the accurate assessment of thermal stability under daily climatic fluctuations and necessitates methodological refinement [1, 2].

The objective of this study is to systematize and formalize an engineering method for calculating the thermal stability of walls with shielded external surfaces by providing a consistent description of radiative-convective heat exchange, air gap ventilation parameters, and the thermophysical behavior of multilayer building envelopes. The proposed model is based on one-dimensional transient heat conduction with equivalent boundary conditions and is oriented toward practical determination of attenuation coefficients, phase shift, and internal surface temperature amplitude. The novelty of the study lies in the unification of calculation relationships for screens of various structural configurations and ventilation regimes, integrated into a compact algorithm suitable for engineering design practice and subsequent software implementation [3, 4].

Hot climates dominate tropical and subtropical regions, where high solar radiation intensity and elevated air temperatures prevail throughout significant parts of the year. Extremely high temperatures have been recorded in arid regions such as the Sahara Desert and Lut Desert, and in locations such as Death Valley, California (USA), where air temperatures have reached 53.7°C. In southern Russia, Central Asia, and southern Kazakhstan, sharply continental climatic conditions lead to prolonged summer overheating periods [5-7].

Most territories of southern Russia, Central Asia, and southern Kazakhstan (excluding mountainous regions) exhibit pronounced arid climate characteristics. The overheating period lasts from 5 to 8 months annually. Solar radiation intensity reaches approximately 1000 W/m<sup>2</sup>, summer air temperatures exceed 40°C, annual sunshine duration exceeds 2000 hours, and air mobility remains relatively low (3-5 m/s) with humidity levels of 25-40%. These conditions frequently cause overheating of residential buildings and urban territories, generating significant thermal loads on occupants and increasing energy demand for cooling [8].

Maintaining a favorable indoor microclimate in southern regions therefore represents a complex engineering challenge due to the diversity of architectural and structural solutions, variability of climatic effects, and the dynamic nature of solar and convective heat transfer processes [9-11].

Modern building science has achieved substantial progress in the field of building climatology. Practical methods for accounting for climatic impacts on the thermal performance of buildings have been developed and are presented in classical foundational studies [Bogoslovsky V.N., Fokin K.F. and Tabunshchikov Y.A. These works provide a scientific and methodological basis for the climatic typology of residential buildings and identify spatial planning and architectural-structural measures that ensure a favorable indoor and urban microclimate (Myagkov M.S., Malyavina, E.G., Shklover, A.M.).

In the design of building envelopes, in addition to structural stability and strength calculations, adequate thermal protection must be ensured. Providing comfortable indoor conditions while minimizing exposure to adverse temperature effects and solar radiation is essential for achieving bioclimatic indoor comfort. The theory of thermal stability has been comprehensively developed in foundational studies. The approaches presented to various aspects of the thermal behavior of building

envelopes and indoor spaces under periodic thermal loading are based on the solution of the differential heat conduction equation for harmonic temperature waves.

In parallel, a number of contemporary researchers have further advanced the theory of thermal protection and thermal stability of building envelopes (Gagarin V.G.). A key factor in determining indoor thermal conditions is the ability of a space to maintain relatively stable temperatures under varying heat gains [11], which characterizes the internal thermal stability of the building [12, 13].

The dependence of the optimal insulation thickness of exterior walls on climatic conditions has been demonstrated in previous studies, but the analysis was limited to established thermal conditions. Other studies have revealed the critical role of climatic characteristics in the design of energy-efficient building enclosing structures, while paying limited attention to local thermal engineering features of specific structural configurations [14]. It was also shown that an increase in thermal mass does not automatically lead to an increase in the energy efficiency of a building, although its inclusion in facade systems has not been considered in detail. A transitional model of the building's thermal regime has been proposed in the literature, taking into account heating systems, but the structural characteristics of the external enclosing structures have been considered only superficially [15]. In addition, the combined effect of thermal insulation and thermal inertia on achieving thermal autonomy was emphasized, but without special consideration of ventilated facade systems. The potential of the building's thermal mass for regulating energy consumption was also investigated, although its interaction with multilayer external enclosing structures remains insufficiently studied [16-18].

Overall, these studies provide engineering methods for evaluating the impact of the external climatic environment on building envelopes and for assessing their thermal response. However, the coupled radiative-convective heat transfer processes occurring within ventilated facade systems, particularly under high solar radiation and significant daily temperature fluctuations, remain insufficiently formalized within practical engineering calculation frameworks.

Ventilated facade systems are currently widely used in both new construction and the renovation of existing buildings. Their extensive application is primarily driven by installation efficiency, technological flexibility, and the relative independence of construction processes from seasonal and weather conditions. Ventilated facades are multilayer envelope systems designed to ensure air circulation between the load-bearing structural wall layer and the external cladding. This configuration promotes effective moisture removal, reduces the risk of condensation, and enhances the overall thermal insulation performance of the building envelope. The principal objective of such facade systems is to maintain a stable and comfortable indoor microclimate while extending the service life of structural elements. In addition to their functional advantages, ventilated facades contribute to architectural expressiveness and the aesthetic modernization of buildings. The proposed engineering method for calculating the thermal stability of walls with shielded external surfaces is grounded in classical heat transfer theory and similarity principles presented in established studies [19].

According to available estimates, approximately 40% of building heat losses and 30-60% of heat gains occur through external walls. Improving the thermal protection performance of building envelopes contributes to reducing heating and cooling energy consumption, enhancing operational efficiency, and extending the service life of structural components. In response to the need to account for climatic conditions in the design and operation of buildings, numerous regulatory and technical standards have been developed and are continuously updated at both national and international levels to improve the thermal performance of building envelopes.

Ventilated facade systems are subject to strict requirements concerning moisture protection, thermal insulation performance, and mechanical resistance. Compliance with applicable building codes and technical standards ensures durability, operational reliability, and safety throughout the service life of the structure.

According to regulatory and technical standards, ventilated wall systems are subject to a range of operational impacts.

Operational impacts include:

1. Thermal effects: temperature gradients between indoor and outdoor environments, as well as cyclic heating and cooling of structural elements.
2. Moisture effects: atmospheric precipitation (rain, snow, hail) and condensation within the ventilated air cavity.

3. B Wind loads: static wind pressure acting on cladding materials and vertical distribution of wind pressure along the building height.

4. Mechanical actions: loads from the self-weight of structural components and dynamic loads (including seismic actions in earthquake-prone regions and accidental loads).

5. Corrosive effects: chemical aggressiveness of the surrounding environment, including acid precipitation and salt exposure.

6. Biological effects: growth of mosses, fungi, and microorganisms on exposed surfaces.

Considering the combined influence of mechanical and non-mechanical environmental actions, compliance with the following performance requirements is essential for ensuring the reliability and long-term performance of ventilated façade systems:

- thermal performance requirements;
- waterproofing and moisture protection requirements;
- durability and maintainability requirements;
- fire safety requirements;
- environmental sustainability requirements.

Depending on structural configuration and architectural design of the cladding system, ventilated façade systems may be classified into several types (Fig. 1).



**Fig. 1.** Cladding panel modules.

The selection of thermal insulation materials is determined by their density, thermal conductivity properties, and vapor barrier characteristics (Fig. 2).

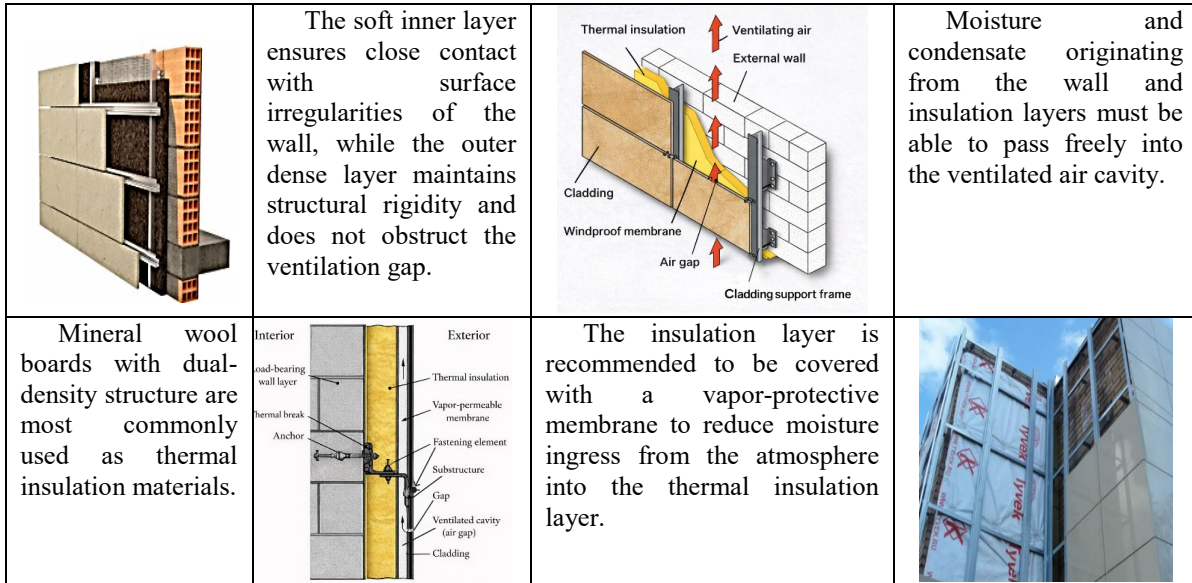


**Fig. 2.** Recommended thermal insulation materials.

The most widely used façade systems are those clad with metallic elements (including standard and custom-designed metal cassette panels), corrugated metal sheets, metal siding, and perforated metal panels manufactured from galvanized or stainless steel, as well as copper- or aluminum-based alloys.

In a ventilated façade system, the structural layers are arranged in the following sequence (from the interior surface to the exterior):

load-bearing wall – thermal insulation layer – air gap – protective screen (cladding).

This configuration is considered optimal, as the material layers located before the air cavity are arranged in order of decreasing thermal conductivity and increasing vapor permeability (Fig. 3).



**Fig. 3.** Configuration of the load-bearing frame of a façade system with vertical profiles.

Вот корректная версия в академическом Scopus-style English:

In the field of innovative ventilated façade technologies, a number of studies have been conducted in recent years [20, 21]. However, the calculation, analysis, and evaluation of ventilated façade systems and their energy performance within the framework of thermal stability theory under dominant climatic thermal loading remain insufficiently investigated.

The objective of this study is to develop a calculation method suitable for engineering design practice for assessing the amplitude attenuation and phase shift of the internal surface temperature of building envelopes under daily climatic fluctuations.

## 2. METHODS AND MATERIALS

The design of ventilated façade systems requires both structural and thermophysical analyses. Thermophysical assessment includes thermal performance calculation, moisture analysis, and evaluation of the air permeability of the building envelope.

In the Russian Federation and the Republic of Kazakhstan, the principal regulatory documents governing the thermal calculation of ventilated façade systems include SP 50.13330.2012, SP 2.04-107-2022, the guidelines for the design of curtain wall systems with ventilated air cavities for new construction and building renovation, and SP 70.13330.2012.

SP 50.13330.2012 provides a methodology for the thermophysical calculation of ventilated façade systems. The thermophysical assessment includes:

- determination of the minimum required insulation thickness for walls with ventilated façades to meet regulatory thermal resistance requirements;
- evaluation of the thermal stability of the building envelope;
- calculation of the moisture regime and verification of material moisture content against regulatory limits;
- calculation of air exchange within the ventilated cavity;
- verification of the adequacy of moisture removal from the air cavity during the design period;
- determination of the required air permeability resistance of the wall assembly.

The present study provides a generalization, analysis, and assessment of the methodology for calculating the thermal stability of walls with ventilated façade systems in regions characterized by hot climates.

In addressing building overheating, consideration of the thermal stability of envelope structures is particularly important, as solar radiation and outdoor temperature effects exhibit pronounced daily periodic fluctuations (Fig. 4).

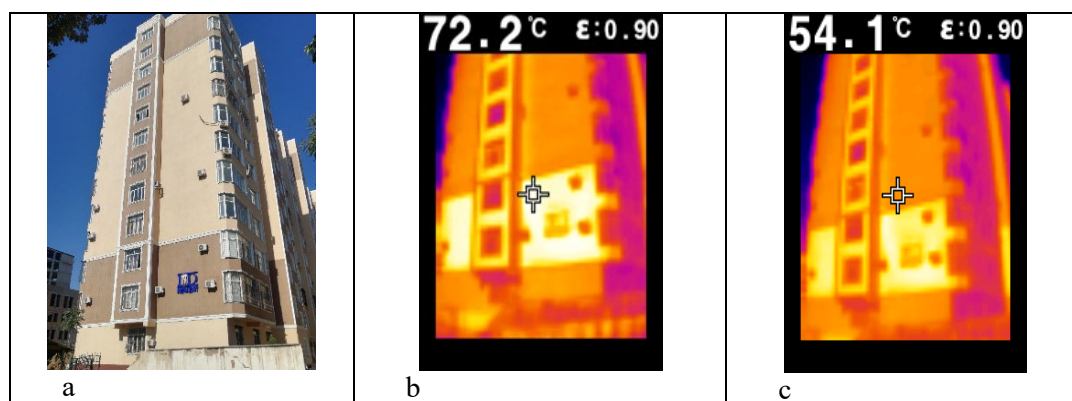


**Fig. 4.** Thermal imaging model of façade walls with western orientation: (a) façade view; (b) thermal condition of the western façade; (c) thermal condition of the eastern façade.

## 3. RESULTS AND DISCUSSION

According to the theory of thermal stability, building envelope structures are subjected to periodically varying ambient air temperatures that follow a cosine function. Field measurements and theoretical investigations demonstrate near-wall air temperature variations under solar exposure of façades with different orientations, forming the basis of modern thermal engineering calculations of building envelopes. These observations form the basis of contemporary thermal engineering calculations of building envelopes.

Based on this theoretical framework, a schematic representation of the amplitude of air temperature fluctuations near the envelope surface, both on the exterior and interior sides, is proposed as the foundation for the theoretical assessment of the thermal stability of ventilated walls (Figure 5). The scheme accounts for the amplitude of fluctuations in ambient air temperature, near-wall air layer temperature, and external and internal wall surface temperatures [15].

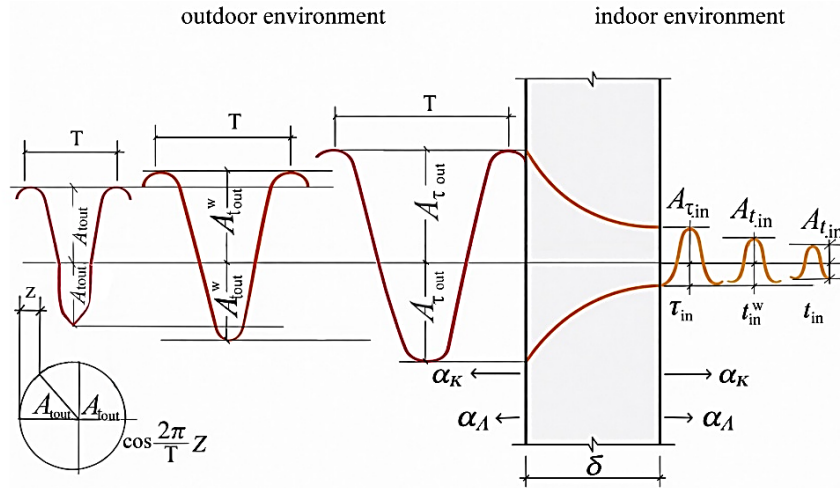


**Fig. 5.** Schematic representation of temperature fluctuation attenuation in the building envelope.

The airflow pattern in ventilated façade systems is presented in Fig. 6.

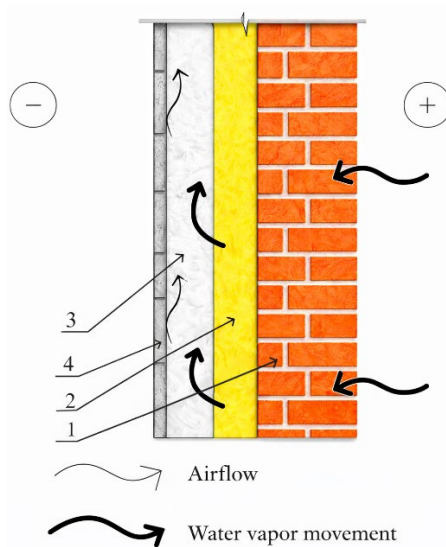


**Fig. 6.** Model of airflow pattern within the building envelope: 1 – insulated wall; 2 – thermal insulation; 3 – ventilated air gap; 4 – external cladding.

The thermal stability of a building envelope is characterized by the degree of attenuation of temperature fluctuations at its internal surface. In envelopes incorporating ventilated air cavities, the magnitude of temperature attenuation depends on the air exchange rate within the cavity. Increasing the intensity of airflow in the air gap promotes the removal of excess heat transmitted through the outer layer behind the screen toward the interior under solar radiation exposure and contributes to cooling of the envelope mass during evening and nighttime periods. Since the structural layer located beneath the ventilated air cavity is often continuous, thermal analysis of ventilated envelope systems

under transient heat transfer conditions can be reduced to determining temperature fluctuations within the air cavity. The attenuation of thermal waves in the envelope mass may be evaluated using either the method. Temperatures at the surfaces of individual layers and within the air cavity, as well as airflow velocity in the cavity, can be determined from a system of heat balance equations under quasi-steady heat transfer conditions. Unlike horizontal envelope systems with ventilated cavities, vertical envelope configurations require a modified approach to determining airflow velocities due to the presence of significant buoyancy-driven pressure differences and the corresponding variation in convective heat transfer coefficients at the bounding surfaces of the cavity.

The proposed calculation model for the thermal engineering assessment is presented in Fig. 7.

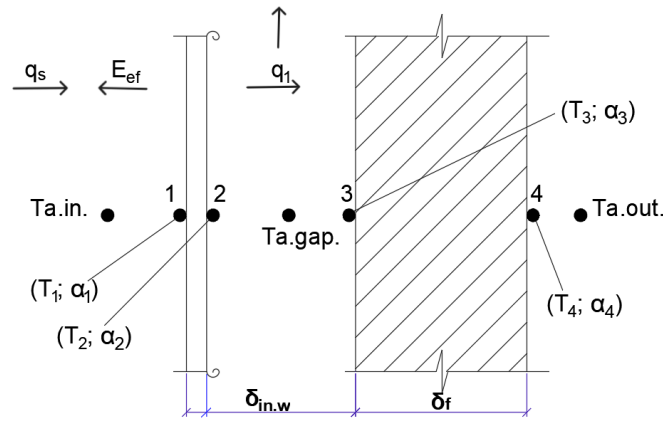


Fig. 7. Calculation model of a ventilated wall.

In the system of equations, the unknown variables are  $\mathcal{L}_a$  and  $T_i$ .

All other parameters are determined using analytical expressions or obtained from tables provided in regulatory and technical standards.

$$A_c q_s + E_{ef} + \alpha_i (T_1 - T_{a.in.}) + (\lambda/\delta)_1 (T_1 - T_2) = 0, \quad (1)$$

$$\alpha_2 (T_2 - T_b^x) + \alpha_\lambda (T_2 - T_3) - (\lambda/\delta)_1 (T_1 - T_2) = 0, \quad (2)$$

$$\alpha_r (T_2 - T_3) + \alpha_3 (T_b - T_3) - (\lambda/\delta)_2 (T_3 - T_4) = 0, \quad (3)$$

$$(\lambda/\delta)_2 (T_3 - T_4) - \alpha_4 (T_4 - T_{a.out.}) = 0, \quad (4)$$

$$\mathcal{L}_a \cdot c_p \cdot dT = (\alpha_2 T_2 + \alpha_3 T_3 + \alpha_2 T_b^x - \alpha_3 T_b^x) dx. \quad (5)$$

The values of the heat transfer coefficients for the internal and external surfaces of the building envelope ( $\alpha_i$  and  $\alpha_e$ ) are adopted in accordance with SP 50.13330 Thermal Protection of Buildings. The convective heat transfer coefficients  $\alpha_2$  and  $\alpha_3$ , based on field experimental studies of envelope systems with ventilated air cavities, are proposed to be determined using the following expression:

$$\alpha_c = 7.34 \cdot (V_{a.gap})^{0.656} + 3.78 \cdot e^{-1.91V_{a.gap}}, \quad (6)$$

The radiative heat transfer coefficient  $\alpha_r$  is calculated as a function of the emissivity of the surfaces bounding the air cavity.

$$\alpha_r = \frac{m}{\frac{1}{\epsilon_1} + \frac{1}{\epsilon_2} + \frac{1}{\epsilon_0}}, \quad (7)$$

$$m = 0.04 \left( \frac{273+t_1}{100} \right)^3, \quad (8)$$

The external surface heat transfer coefficient under summer conditions,  $\alpha_e$  (W/(m<sup>2</sup>·K)), shall be determined in accordance with SP 50.13330 using the following expression

$$\alpha_{\text{out}} = 1.16(5 + 10\sqrt{v}) \cdot \quad (9)$$

The convective heat transfer coefficient of the external surface under calm weather conditions is determined by the thermophysical properties of the surrounding medium, heat transfer conditions (airflow velocity and buoyancy effects), as well as geometric parameters. It can be calculated using dimensionless similarity numbers, such as the Reynolds number (Re) and the Nusselt number (Nu), together with appropriate empirical correlation equations.

A theoretical calculation based on the proposed thermal stability methodology was performed for a three-layer wall of a building located in Shymkent. The wall had a total thickness of 0.20 m and consisted of an external reinforced concrete layer (density  $\rho = 2500 \text{ kg/m}^3$ , thickness  $\delta = 0.03 \text{ m}$ ), a mineral wool insulation layer ( $\rho = 125 \text{ kg/m}^3$ ,  $\delta = 0.16 \text{ m}$ , thermal conductivity  $\lambda = 0.045 \text{ W/(m}\cdot\text{K)}$ ), and an internal cement-sand plaster layer ( $\rho = 1800 \text{ kg/m}^3$ ,  $\delta = 0.01 \text{ m}$ ). To investigate the thermal protection performance of shielded walls and to develop rational screen configurations, summer field studies were conducted in Shymkent in a commissioned nine-story frame residential building with load-bearing walls 0.20 m thick.

For the experimental investigation, four west-oriented rooms were selected in standard apartments located on the 6<sup>th</sup>, 7<sup>th</sup>, 8<sup>th</sup>, and 9<sup>th</sup> floors, vertically aligned above one another. To provide external shading, four solar protection screens were fabricated (three solid-type screens and one louver-type screen). The solid screens were coated with aluminum having high reflectivity (solar absorptivity coefficient  $\rho_s = 0.2\text{-}0.3$ ). When mounted on the external wall surface, a ventilated air cavity with a thickness of 50 mm was formed. The louver-type screen consisted of a supporting frame with plastic strips 10 cm in width serving as shading elements. During the first stage of the study, a louver-type screen with dimensions corresponding to one façade panel ( $3.3 \times 3.0 \text{ m}$ ) was installed in front of the wall on the 6<sup>th</sup> floor. In the second stage, it was replaced with a solid-type screen. In the third stage, three solid-type screens were mounted vertically on the upper floors, one above another, with the ventilated air cavity extended to the building roof. At intervals of 1.5 m, temperatures of the outdoor air, the external and internal surfaces of the screen, the air within the cavity, and the wall surfaces were measured using copper-constantan thermocouples. In addition, wind velocity and airflow velocity within the ventilated cavity were recorded. Measurements at all stages were conducted at hourly intervals over a 24-hour period.

The results demonstrated that the application of shielded façade systems reduces the amplitude of internal wall surface temperature fluctuations by a factor of 1.5-2 and ensures stable thermal comfort under peak solar radiation conditions. Comparison of field measurement data with theoretical predictions obtained using the developed engineering methodology confirmed the high accuracy of the proposed model: the discrepancy between experimental and calculated results did not exceed 5-10%. The obtained results are consistent with full-scale field studies conducted under hot climate conditions, confirming that natural convection within a 50 mm air cavity, combined with a low-emissivity screen surface, effectively mitigates radiative overheating of external walls and reduces the thermal load on the building air-conditioning system.

In the development of the engineering method for calculating the thermal stability of walls with shielded external surfaces, based on heat transfer theory, the following aspects were investigated:

- analysis of the aerodynamic airflow regime within ventilated wall cavities based on literature sources and experimental data;
- determination of thermophysical parameters describing heat transfer processes through the air cavity;
- development of an engineering method for evaluating the thermal stability of ventilated walls;
- validation of the proposed method through comparison of calculated results with experimental measurements.

Airflow within a ventilated cavity is analogous to flow in plane vertical channels. Based on the processing of extensive experimental data on convective heat transfer in channels, Mikheev M.A. proposed a dimensionless correlation, which for air can be written as:

$$N_{\text{air}} = 0.018Re^{0.80}\epsilon h \cdot \quad (10)$$

By expanding correlation (10) and performing the corresponding transformations, an expression was obtained for determining the convective heat transfer coefficient in the air cavity.

Under summer conditions, the screen is heated due to elevated outdoor air temperature and solar radiation exposure and transfers heat to the shaded wall surface by radiation and convection through the ventilated air cavity.

Heat transfer through a wall incorporating a ventilated air cavity may be considered as a combined heat transfer process by introducing an effective thermal conductivity of air,  $\lambda_{eff}$ , which accounts for both convective and radiative components of heat transfer.

From the heat balance equations for the wall, substituting the corresponding parameters and performing the necessary transformations, the following expression was obtained for determining the effective thermal conductivity  $\lambda_{eff}$ :

$$\lambda_{eff} = 0.06\alpha_k + 0.68\epsilon h. \quad (11)$$

Having determined the values of  $\alpha_c$  and  $\lambda_{eff}$  the thermal stability of ventilated walls can be evaluated based on the fundamental principles of the engineering method proposed by V.N. Bogoslovsky.

The overall attenuation coefficient of the envelope is defined as the product:

$$v = v_{out} v_{sc} v_{a,gap} v_w. \quad (12)$$

The expressions for determining  $v_{out}$  and  $v_w$  are provided in the aforementioned methodology. The coefficients  $v_{sc}$  and  $v_{a,gap}$  re determined using the following relationships:

$$v_{sc} = e^{-\frac{R_{sc} S_{sc}}{\sqrt{2}}} \cdot \frac{S_{sc} + \alpha_l}{S_{sc} + Y_{sc}}; \quad v_{a,gap} = e^{-\frac{R_{a,gap} S_{a,gap}}{\sqrt{2}}} \cdot \frac{\alpha_{a,gap} + Y_w}{\alpha_{a,gap} + Y_{a,gap}};$$

$$R_{a,gap} = \frac{\delta_{a,gap}}{\lambda_{eff}}; \quad Y_{a,gap} = \frac{Y_w}{1 + R_{a,gap} Y_w}. \quad (13)$$

Airflow within the ventilated cavity is driven by buoyancy (thermal draft) and wind pressure. When the inlet and outlet openings are located on different walls, the air velocity in the cavity  $V_{a,gap}$  can be determined as:

$$V_{a,gap} = \sqrt{\frac{K(K_{out} - K_3) V_{out}^2 + 0.08h(\tau_{a,gap} - \tau_{out})}{\sum_i \xi_i}}. \quad (14)$$

If the inlet and outlet openings of the air cavity are located on the same façade, the coefficient  $K_{out} = K_3$ , and expression (14) simplifies to:

$$V_{a,gap} = \sqrt{\frac{0.08h(\tau_{a,gap} - \tau_{out})}{\sum_i \xi_i}}. \quad (15)$$

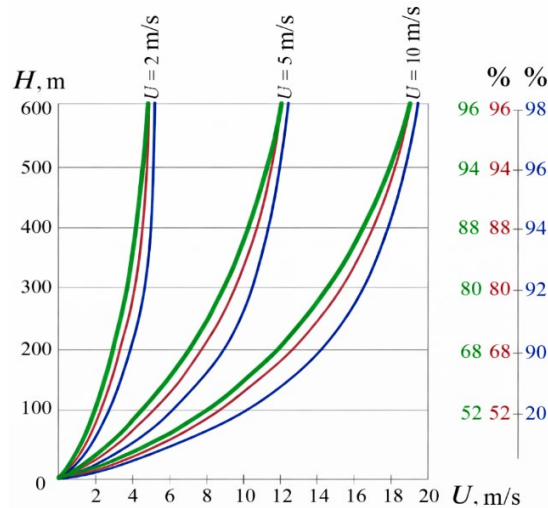


**Fig. 8.** Variation of wind velocity with height: blue line – suburban areas; red line – urban areas with an average building height up to 100 m; green line – urban areas with an average building height exceeding 100 m.

The study provides expressions for determining the components of equations (16) and (17). The calculation is performed using an iterative procedure. The coefficients  $K_1$  and  $K_2$  were determined through experimental investigations on building models tested in a wind tunnel. The theoretical basis of the model experiments is the theory of similarity. Issues of aerodynamic similarity have been extensively studied, and it is generally accepted that the flow around rectangular bodies remains largely independent of the Reynolds number over a wide range. Thus, the phenomenon exhibits self-similarity, allowing the results obtained from model testing to be reliably extrapolated to full-scale structures.

The study was conducted using wind tunnel testing of residential building models. The models were manufactured at a scale of 1:50 to ensure self-similarity and to investigate the influence of thermal processes on the wind regime of urban development. The wind tunnel facility enables the analysis of aerodynamic behavior of buildings and residential development areas under controlled conditions.

Aerodynamic coefficients are determined either experimentally through wind tunnel testing of building models or analytically using the geometric criterion.

Models corresponding to square-plan residential buildings with side lengths of 24 m and a height of 60 m were investigated. The models incorporated a shielded façade configuration, with the air inlet to the ventilated cavity located at the level of the floor slab between the first and second stories, and the exhaust outlet positioned at roof level. Measurements were carried out for five design wind directions relative to the shielded façades of the models:  $0^\circ$ ,  $45^\circ$ ,  $90^\circ$ ,  $225^\circ$ , and  $270^\circ$ . Fig. 8 presents an example of the vertical distribution of aerodynamic coefficients along the surfaces of a square-plan building model for a wind direction of  $90^\circ$ .

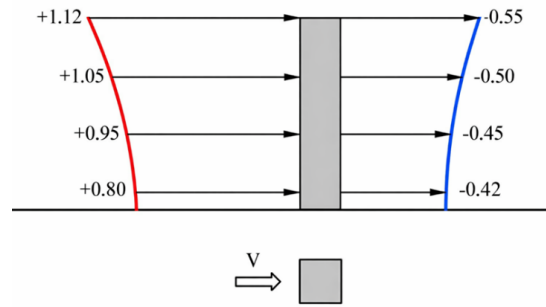


**Fig. 9.** Vertical distribution of aerodynamic coefficients along the surfaces of a square-plan building model: coefficients are positive on the windward wall and negative on the leeward wall.

Processing of the experimental data made it possible to propose analytical expressions for determining aerodynamic coefficients, which can be reliably applied in thermal stability calculations of ventilated building envelope systems.

Based on wind tunnel testing of isolated building models with various geometric parameters, empirical formulas were derived for calculating aerodynamic coefficients for buildings with unfavorable orientation (perpendicular to the wind flow):

For the windward wall of the building:

$$K_{90}^+ = \frac{0.064}{z_{90}^+} + 0.435 \cdot \quad (16)$$

For the leeward wall:

$$K_{90}^- = \frac{0.043}{z_{90}^-} + 0.342 \cdot \quad (17)$$

The proposed analytical expressions, derived from the developed building aeration methodology, allow determination of aerodynamic coefficients at different height levels of building models while accounting for wind velocity variation with height. This approach enables more accurate estimation of wind velocity and aerodynamic coefficients at the inlet and outlet of the screen.

In expressions (14) and (15), the concept of the average air temperature in the cavity,  $t_{a,gap}$ , is introduced. This temperature depends on the airflow velocity within the ventilated cavity and is determined as follows:

$$t_{a,gap} = t_0 - (t_0 - t_{out}) \cdot \frac{x_0}{h} \cdot \left[ 1 - \exp\left(-\frac{h}{x_0}\right) \right], \quad (18)$$

where

$$t_0 = \frac{\frac{t_{in}}{R_{in}} + \frac{t_{out}}{R_{out}}}{\frac{1}{R_{in}} + \frac{1}{R_{out}}}, \quad (19)$$

is the limiting air temperature in the cavity, expressed in °C.

$$x_0 = \frac{C_a \cdot V_{a,gap} \cdot \delta_{a,gap} \cdot \rho_a}{\frac{1}{R_{in}} + \frac{1}{R_{out}}}, \quad (20)$$

Here,  $x_0$  represents the characteristic height (m) at which the air temperature in the cavity becomes lower than the limiting temperature  $t_0$  by a factor of  $e$  (where  $e \approx 2.7$ ) relative to the inlet temperature.

During the investigation, variations in air temperature within the cavity were observed; however, the temperature coefficient exhibited only minor variability. Therefore, its value is determined once at the initial stage of the calculation for the temperature  $t_{out} + I$ .

The temperature and velocity parameters of the airflow within the cavity are determined using an iterative procedure.

At the first stage, the average air temperature in the cavity is calculated using equation (18), taking into account the heat transfer coefficient  $\alpha_{a, gap}$ . Subsequently, the average airflow velocity in the cavity is determined using equations (14) or (15) for the specified temperature conditions. The heat transfer coefficient in the cavity and the thermal resistance  $R_{out}$  are then recalculated. Using equation (18), a new value of the average air temperature in the cavity is obtained based on the updated airflow velocity. The iterative process continues until the difference between airflow velocities in successive iterations becomes less than 5%.

At the initial stage of the iterative procedure, the average airflow velocity in the cavity is assumed to be 0 m/s. As a result of the calculations, the air temperature and airflow velocity in the cavity, as well as the corresponding heat transfer coefficient  $\alpha_{a, gap}$  are determined.

The total vapor diffusion resistance of the wall is defined as the sum of the vapor resistance values of all structural layers plus the surface moisture transfer resistances at the internal and external boundaries. The air permeability of the structure shall not exceed the required limit.

#### 4. CONCLUSIONS

The thermal protection performance of screens of different configurations was evaluated by comparing the average and maximum air temperatures within the ventilated cavity with the corresponding temperatures at the wall surfaces.

The results demonstrate that façade screening is an effective means of enhancing the thermal stability of building envelopes. The close agreement between the maximum air temperatures in the cavity and those measured on shaded wall surfaces indicates that direct solar radiation is effectively eliminated and that the thermal regime of the wall approaches shaded conditions.

The nearly identical differences between maximum and average temperatures in the cavity and the corresponding surface temperatures indicate a similar pattern of convective flow formation and, consequently, comparable thermal protection performance of the examined screen types. Statistical analysis of monitoring data and calculated temperature profiles showed that the difference in heat removal efficiency between solid screens and louver-type screens does not exceed 3-5%. Preference may be given to solid screens due to their structural simplicity and lower material consumption compared to louver-type configurations.

When solid-type screens are used and the air cavity exhaust is located at roof level, the airflow velocity within the ventilated cavity is predominantly governed by wind pressure. Investigation of the aerodynamic regime revealed that airflow is mainly forced in nature and predominantly turbulent.

No systematic increase in shaded wall surface temperature with height was observed. The airflow within the cavity, characterized by relatively high velocities (0.7 m/s at Stage I, 1.22 m/s at Stage II, and 1.33 m/s at Stage III), did not allow significant air heating. The differences between maximum temperatures at the outlet and inlet of the cavity were only 0.2°C at Stages I and II and 1°C at Stage III.

The analysis indicates that previously developed methods for calculating the thermal stability of external envelopes cannot be fully applied to ventilated wall systems due to insufficient consideration of the aerodynamic and temperature regimes of walls with shielded external surfaces.

Despite higher initial installation costs, ventilated façade systems demonstrate high economic efficiency due to reduced heating and air-conditioning energy consumption. Practical implementation examples confirm significant reductions in operational costs achieved through the use of such systems.

The proposed enhanced algorithm for evaluating thermal stability can be widely applied in design practice, including the selection of insulation thickness for external envelope systems in southern regions, determination of design loads for ventilation and air-conditioning systems, and assessment of indoor thermal regimes under intermittent heating and ventilation conditions.

5. ACKNOWLEDGEMENTS

This research is funded by the Science Committee of the Ministry of Science and Higher Education of the Republic of Kazakhstan (Grant No. AP23486892).

Appendix

|                          |   |
|--------------------------|---|
| $q_s$                    | intensity of solar radiation incident on a vertical surface, W/m <sup>2</sup>   |
| $E_{ef}$                 | effective heat flux from the external surface, W/m <sup>2</sup>   |
| $\alpha_i$               | heat transfer coefficient at the i-th surface, W/(m <sup>2</sup> ·K)  |
| $\alpha_r$               | radiative heat transfer coefficient between the screen and the envelope surface, W/(m <sup>2</sup> ·K)                      |
| $c_a$                    | specific heat capacity of air, J/(kg·K)   |
| $x$                      | current air path length within the cavity, m  |
| $\mathcal{L}_a$          | mass flow rate of air, kg/h   |
| $T_{a,in}$               | indoor air temperature, °C  |
| $T_{a,out}$              | outdoor air temperature, °C   |
| $T_{a,gap}$              | air temperature in the ventilated cavity, °C  |
| $V_{a,gap}$              | air velocity in the cavity, m/s   |
| $C_0$                    | radiation constant of a black body, W/(m <sup>2</sup> ·K <sup>4</sup> )   |
| $C_1, C_2$               | radiation coefficients of surfaces, W/(m <sup>2</sup> ·K <sup>4</sup> )   |
| $m$                      | temperature coefficient   |
| $\alpha_{out}$           | external surface heat transfer coefficient, W/(m <sup>2</sup> ·K)   |
| $\alpha_{in}$            | internal surface heat transfer coefficient, W/(m <sup>2</sup> ·K)   |
| $v$                      | minimum of average wind velocities by compass direction for July, m/s   |
| $\rho$                   | material density, kg/m <sup>3</sup>   |
| $\lambda$                | thermal conductivity of material, W/(m·K)   |
| $\varepsilon_h$          | correction factor depending on the ratio of cavity height $h$ to the equivalent horizontal cross-section area of the cavity |
| $v_{out}$                | attenuation factor for thermal wave transfer from outdoor air to the outer screen surface                                   |
| $v_{sc}$                 | attenuation factor for thermal wave transfer through the screen   |
| $v_{a,gap}$              | attenuation factor for thermal wave transfer through the ventilated air cavity  |
| $v_w$                    | attenuation factor for thermal wave transfer through the wall material layers   |
| $R_{sc}, R_{a,gap}$      | thermal resistances of the screen and air cavity, m <sup>2</sup> ·K/W   |
| $S_{sc}$                 | thermal effusivity coefficient of the screen material   |
| $Y_{sc}, Y_w, Y_{a,gap}$ | thermal effusivity coefficients of the screen, wall, and air cavity surfaces  |
| $K_{out}, K_3$           | aerodynamic coefficients  |
| $K$                      | coefficient accounting for wind velocity variation with height  |
| $h$                      | vertical distance between the air inlet and outlet in the cavity, m   |
| $t_{a,gap}, t_{out}$     | average air temperature in the cavity, °C; outdoor air temperature, °C  |
| $\sum_i \xi_i$           | sum of friction loss coefficients and local resistance coefficients   |
| $B, H, S$                | building width, height, and length, m   |
| $Z$                      | dimensionless geometric simplex   |
| $(\bar{B}), (\bar{S})$   | relative width and height of the building   |
| $\bar{t}_{a,gap}$        | average air temperature in the cavity, °C   |
| $\bar{t}_0$              | limiting air temperature in the cavity, °C  |
| $c_a$                    | specific heat capacity of air, J/(kg·K)   |
| $\rho_a$                 | average air density in the cavity, 353/(273+t <sub>avg</sub> ) kg/m <sup>3</sup>  |
| $R_{out}$                | thermal resistance of the wall from the air cavity to the outdoor environment, m <sup>2</sup> ·K/W                          |
| $R_f$                    | thermal resistance of the cladding layer, m <sup>2</sup> ·K/W   |
| $T$                      | period of temperature fluctuations  |
| $Z$                      | depth (coordinate) of temperature wave propagation within the envelope, m   |
| $A_{\tau,out}$           | amplitude of outdoor air temperature fluctuations, °C   |

|                 |   |
|-----------------|---|
| $A_{t_{out}}^w$ | amplitude of temperature fluctuations in the external near-wall air layer, °C     |
| $A_{r_{out}}$   | amplitude of temperature fluctuations at the external surface of the envelope, °C |
| $A_{r_{in}}$    | amplitude of temperature fluctuations at the internal surface of the envelope, °C |
| $A_{t_{in}}^w$  | amplitude of temperature fluctuations in the internal near-wall air layer, °C     |
| $A_{t_{in}}$    | amplitude of indoor air temperature fluctuations, °C                              |
| $a_k$           | convective heat transfer coefficient, W/(m <sup>2</sup> ·K)                       |
| $a_d$           | radiative heat transfer coefficient, W/(m <sup>2</sup> ·K)                        |
| $\delta$        | thickness of the envelope layer, m  |
| $\tau_{in}$     | phase shift of the temperature wave at the internal surface                       |
| $t_{in}^w$      | temperature of the internal near-wall air layer, °C                               |
| $t_{in}$        | indoor air temperature, °C  |

## REFERENCES

1. De Masi R., Ruggiero S., Vanoli P. Hygro-thermal performance of an opaque ventilated façade with recycled materials during wintertime. *Energy & Buildings*. 2021. 245. P. 110994. DOI: <https://doi.org/10.1016/j.enbuild.2021.110994>
2. Kumar V.V., Raut, N., Akeel, N.A. et al. Experimental investigation of cooling potential of a ventilated cool roof with air gap as a thermal barrier. *Environ Dev Sustain*. 2023. 25. P. 3255 – 3268. DOI: <https://doi.org/10.1007/s10668-022-02184-y>
3. Pajek L., Potočnik J., Košir M. The effect of a warming climate on the relevance of passive design measures for heating and cooling of European single-family detached buildings. *Energy and Buildings*. 2022. 261 (6). P. 111947. DOI: <https://doi.org/10.1016/j.enbuild.2022.111947>
4. Pajek L., Košir M. Strategy for achieving long-term energy efficiency of European single-family buildings through passive climate adaptation. *Applied Energy*. 2021. 297. P.117116. DOI: <https://doi.org/10.1016/j.apenergy.2021.117116>
5. Perkins-Kirkpatrick S.E., Lewis S.C. Increasing trends in regional heatwaves. *Nat Commun*. 2020. 11. P. 3357. DOI: <https://doi.org/10.1038/s41467-020-16970-7>
6. Liu Q., Fu C., Xu Z. Global warming intensifies extreme day-to-day temperature changes in mid–low latitudes. *Nature Climate Change*. 2026. 16. P. 69 – 76. DOI: <https://doi.org/10.1038/s41558-025-02486-9>
7. Adeyeri O.E., Ishola K.A., Ajadi S.A. Coupled climate–land-use interactions modulate projected heatwave intensification across Africa. *Communications Earth & Environment*. 2026. 7. P. 85 DOI: <https://doi.org/10.1038/s43247-025-03110-6>
8. Al-Awadi H., Alajmi A., Abou-Ziyan H. Effect of Thermal Bridges of Different External Wall Types on the Thermal Performance of Residential Building Envelope in a Hot Climate. *Buildings*. 2022. 12. 312. DOI: <https://doi.org/10.3390/buildings12030312>
9. Zhangabay N., Tursunkululy T., Ibraimova U., Abdikerova U. Energy-Efficient Adaptive Dynamic Building Facades: A Review of Their Energy Efficiency and Operating Loads. *Applied Science*. 2024. 14. 10979. DOI: <https://doi.org/10.3390/app142310979>
10. Zhangabay N., Zhangabay A., Utelbayeva A., Tursunkululy T., Sultanov M., Kolesnikov A. Energy-Efficient Outdoor Fencing with Air Layers: A Review of the Effect of Solar Radiation on the Exterior Fencing of Buildings Made of Composite Material. *Journal of Composites Science*. 2025. 9. 9. DOI: <https://doi.org/10.3390/jcs9010009>
11. Zhangabay N., Tagybayev A., Utelbayeva A., Buganova S., Tolganbayev A., Tulesheva G., Jumabayev A., Kolesnikov A., Kambarov M., Imanaliyev K., Kozlov P. Analysis of the influence of thermal insulation material on the thermal resistance of new facade structures with horizontal air channels. *Case Studies in Construction Materials*. 2023. 18. P. e02026. DOI: <https://doi.org/10.1016/j.cscm.2023.e02026>

12. Belous A.N., Belous O.E., Kulumbegova L.Z., Krakhin S.V. Thermal stability of external building envelopes with thermally conductive inclusions during the summer period. *Bulletin of Tomsk State University of Architecture and Building*. 2021. 6 (23). P. 129 – 142. <https://vestnik.tsuab.ru/jour/article/view/1121/783>
13. Chen L., Zhang Y., Zhou X. A new method for measuring thermal resistance of building walls and analyses of influencing factors. *Construction and Building Materials*. 2023. 3 (385). 131438. DOI: <https://doi.org/10.1016/j.conbuildmat.2023.131438>
14. Yari M., Kalbasi R., Thi N.H. Afrand M. Incorporating pcms and thermal insulation into building walls and their competition in building energy consumption reduction. *Case Studies in Thermal Engineering*. 2024. 63. 105398. DOI: <https://doi.org/10.1016/j.csite.2024.105398>
15. Elmezghi M., Alghoul S., Mashena M. Optimizing thermal insulation of external building walls in different climate zones in Libya. *Journal of Building Physics*. 2021. 3 (45). P. 368 – 390. DOI: <https://doi.org/10.1177/1744259120980027>
16. Zhangabay N., Giyasov A., Ibraimova U., Tursunkululy T., Kolesnikov A. Construction and climatic certification of an area as a prerequisite for development of energy-efficient buildings and their external wall constructions. *Construction materials and products*. 2024. 7 (5). P. 1 – 17. DOI: <https://doi.org/10.58224/2618-7183-2024-7-5-1>
17. Pereira C., Silva A., de Brito J., D. Silvestre J. Urgency of repair of building elements: Prediction and influencing factors in façade renders. *Construction and Building Materials*. 2020. 249. P. 118743. DOI: <https://doi.org/10.1016/j.conbuildmat.2020.118743>
18. Gunawardena K., Kershaw T., Steemers K. Simulation pathway for estimating heat island influence on urban/suburban building space-conditioning loads and response to facade material changes. *Building and Environment*. 2019. 150. P. 195 – 205. DOI: <https://doi.org/10.1016/j.buildenv.2019.01.006>
19. Rajagopal P., Priya R.Sh., Senthil R. A review of recent developments in the impact of environmental measures on urban heat island. *Sustainable Cities and Society*. 2023. 88. P. 104279. DOI: <https://doi.org/10.1016/j.scs.2022.104279>
20. Cuce P.M., Cuce E. Ventilated Facades for Low-Carbon Buildings: A Review. *Processes*. 2025. 13. 2275. DOI: <https://doi.org/10.3390/pr13072275>
21. Vakhrushev K.G., Simachkov M.A. Modular ventilated façades for high-rise construction. *Industrial and Civil Engineering*. 2022. 10. P. 37 – 44. DOI: <https://doi.org/10.33622/0869-7019.2022.10.37-44>

### INFORMATION ABOUT THE AUTHORS

**Zhangabay N.Zh.**, e-mail: [Nurlan.Zhanabay777@mail.ru](mailto:Nurlan.Zhanabay777@mail.ru), ORCID ID: <https://orcid.org/0000-0002-8153-1449>, SCOPUS: <https://www.scopus.com/authid/detail.uri?authorId=57211557292>, M. Auezov South Kazakhstan University, Department of Architecture and Urban Planning, Candidate of Technical Sciences (PhD), Associate Professor

**Giyasov A.I.**, e-mail: [adham52@mail.ru](mailto:adham52@mail.ru), ORCID ID: <https://orcid.org/0000-0002-5982-8983>, SCOPUS: <https://www.scopus.com/authid/detail.uri?authorId=57202817395>, Moscow State University of Civil Engineering (MGSU), Department of Architectural and Construction Design and Environmental Physics, Doctor of Engineering Sciences (Advanced Doctor), Professor

**Zhangabay A.Zh.**, e-mail: [4izhan.ss@gmail.com](mailto:4izhan.ss@gmail.com), ORCID ID: <https://orcid.org/0009-0003-3569-0531>, SCOPUS: <https://www.scopus.com/authid/detail.uri?authorId=59224232100>, Satbayev University, Satbayev, Department of Construction and Building Materials, Doctoral Student

**Kolesnikov A.S.**, e-mail: [kas164@yandex.kz](mailto:kas164@yandex.kz), ORCID ID: <https://orcid.org/0000-0002-8060-6234>, SCOPUS: <https://www.scopus.com/authid/detail.uri?authorId=57189499212>, M. Auezov South Kazakhstan University, Department of Life Safety and Environmental Protection, Candidate of Technical Sciences (PhD), Professor

**Utelbayeva A.B.**, e-mail: [mako\\_01-777@mail.ru](mailto:mako_01-777@mail.ru), ORCID ID: <https://orcid.org/0000-0002-4771-9835>, SCOPUS: <https://www.scopus.com/authid/detail.uri?authorId=57151414400>, M. Auezov South Kazakhstan University, Department of Chemistry, Doctor in Chemistry (Advanced Doctor), Associate Professor